Large impact of coarse-resolution atmospheric transport model error on land-ocean and tropic-extratropic partitioning and seasonal cycle in CO_2 inversion

Zhiqiang Liu[1,2], Ning Zeng[3,4], Pengfei Han[5,1], Qixiang Cai[1]

[1]Laboratory of Numerical Modeling for Atmospheric Sciences & Geophysical Fluid Dynamics, Institute of Atmospheric Physics, Chinese Academy of Sciences, Beijing, China

[2]University of Chinese Academy of Sciences, Beijing, China

[3]Dept. of Atmospheric and Oceanic Science, University of Maryland, USA

[4]Earth System Science Interdisciplinary Center, University of Maryland, USA

[5]Carbon Neutrality Research Center, Institute of Atmospheric Physics, Chinese Academy of Sciences, Beijing, China

Corresponding authors: Zhiqiang Liu (liuzhiqiang@mail.iap.ac.cn)

Key Points:

- Error from the coarse-resolution atmospheric transport model can introduce systematic biases to CO_2 modeling and inversed flux estimates.
- The coarse-resolution transport error leads to stronger land and extratropical sink estimates and weaker ocean and tropical sink estimates.
- The error also induces an underestimated seasonal amplitude and a reversed seasonal phase in the northern land and ocean, respectively.

Abstract

We show that forward simulations of global CO_2 using an atmospheric transport model (ATM) at 0.5° ×0.625° and 4° ×5° resolutions differ significantly in vertical and meridional distribution. Comparing two observing simulation system experiments at 4° ×5° resolution that assimilate pseudo observations sampled from the two forward simulations, we isolated the impact of coarse-resolution ATM error on regional flux estimates that a significant amount of annual carbon uptake from the ocean and tropics is improperly redistributed to the land and extratropics, respectively. In addition, this error leads to an underestimated seasonal amplitude in the northern extratropical land and a reversed seasonal phase in the northern extratropical ocean. The reversed seasonal phase has also been shown in a real data assimilation experiment and state-of-the-art inversions, suggesting that ocean glint retrieval error may not be as significant as previously thought and reasonable ocean flux estimates depend strongly on the accuracy of ATM.

Plain Language Summary

Credible regional carbon budget estimates from atmospheric CO_2 measurements rely on the accuracy of atmospheric transport models (ATMs). However, the simulated atmospheric vertical motions in ATMs are usually simplified and spatiotemporally averaged, leading to systematic biases in simulating the long-lived atmospheric CO_2 and estimating surface carbon fluxes. Even though the atmospheric approach is increasingly applied to account for country-level carbon budget in global synthesis activities. Our finding suggests that current coarse-resolution ATMs lead to improper attribution of annual carbon uptake from the ocean and tropics to the land and extratropics, respectively, resulting in overestimated natural carbon uptake and reduced emissions reduction duty in most advanced countries that target carbon neutrality. Furthermore, since the seasonal variation of carbon flux in the ocean is much smaller than in the land, the results indicate that a small seasonal bias from the land can overwrite and even reverse the real flux signal in the ocean.

1 Introduction

Quantifying the country-level CO_2 budget using atmospheric CO_2 inversion technique is one of the critical approaches in the upcoming Global StockTake assessment (Chevallier, 2021; Jiang et al., 2022; Weir et al., 2022; Deng et al., 2022; Byrne et al., 2023). However, several fundamental issues in CO_2 inversion (e.g., transport, satellite retrieval, and a priori errors) have not been fully addressed, challenging the derivation of robust regional CO_2 budget estimation (Fu et al., 2021; O'Dell et al., 2018; Philip et al., 2019; Schuh et al., 2019). Inversion systems use an offline atmosphere transport model (ATM) to relate the surface land and ocean carbon fluxes with observed CO_2 concentration. An offline ATM is driven by the meteorology reanalysis data generated from a general circulation model (GCM), which significantly reduces the computational cost but simplifies and spatiotemporally averages some nonlinear atmospheric processes (J. Liu et al., 2011; Basu et al., 2018; Schuh et al., 2019). The averaging processes include remapping the GCM output from seconds to hours and irregular grid to latitude-longitude grid, and spatial interpolation from native to coarse horizontal resolution, which induces underestimated transient vertical motion and reduced vertical transport (Yu et al., 2018). Recent forward modeling studies find that the simulated CO_2 concentrations are significantly different in vertical and meridional distribution using different ATM configurations and ATMs (Schuh et al., 2019; Schuh & Jacobson, 2022). These biases can influence the estimates of regional carbon budgets (Wang et al., 2020; Schuh et al., 2022) and seasonal cycles (Cui et al., 2022) estimates. A large discrepancy between the inversion estimates and process understandings is the land-ocean and tropic-extratropic partitioning of carbon fluxes. The inversions usually estimate a large carbon sink in the northern extratropics and a weak carbon sink or carbon source in the tropics recently, while process models or inventories suggest more carbon uptake in the tropics (Schimel et al., 2015; Friedlingstein et al., 2022). Evidence from the vertical CO_2 observation profiles indicates that inversions may overestimate the northern sink and underestimate the tropical sink (Stephens et al., 2007).

To reduce the main transport error, running global inversions at the native resolution is a straightforward strategy. However, native resolution inversions can be very slow due to reading and writing a large amount of data and poor parallel methods in some ATMs (e.g., classic GEOS-Chem) (The International GEOS-Chem User Community, 2021). For example, forward simulation of global CO_2 at a native horizontal resolution of 0.5° ×0.625° using GEOS-Chem requires around 60 gigabytes (GB) of memory and could be paralleled using OpenMP only that a one-year simulation costs more than 1 week using 1 Central Processing Unit (CPU) with 20 cores. The computation costs will increase dramatically by at least an order of magnitude when conducting ensemble or adjoint simulation, thus not possible in real inversion applications but acceptable in simple forward simulation. In this study, instead of conducting native inversion directly, we, for the first time, derived the impact of coarse resolution transport model error on large-scale flux distribution in the context of observing simulation system experiments (OSSEs) and further suggested that the estimated northern ocean fluxes in current state-of-the-art inversion systems are likely driven by the transport error instead of observation information or satellite retrieval errors. Section 2 describes the data and method; Section 3 shows the results; the conclusion and discussion are presented in the last section.

2 Data and method

We use the Carbon in Ocean-Land-Atmosphere (COLA) system (Z. Liu et al., 2022, 2023) to understand the transport impact on flux estimation in the context of Observing Simulation System Experiments (OSSEs) and a real data assimilation experiment. COLA optimizes the land (F_{TA}) and ocean (F_{OA}) carbon fluxes using a local ensemble transform Kalman filter and a constrained ensemble Kalman filter, while terrestrial fire flux (F_{IR}) and anthropogenic fossil fuel emissions (F_{FE}) are not optimized. The atmosphere transport model used in COLA is GEOS-Chem of version 13.0.2, driven by the Modern-Era Retrospective analysis for Research and Applications Version 2 (MERRA-2) meteorology reanalysis (Gelaro et al., 2017; The International GEOS-Chem User Community, 2021). The native spatial resolution of MERRA-2 is 0.5° ×0.625°.

In this study, two sets of OSSEs are performed from December 2014 to the end of 2015. In the first OSSE (EXP-biased), the assimilation run is conducted at 4° ×5° resolution while the nature run is conducted at the native 0.5° ×0.625° resolution. In the second OSSE (EXP-perfect), both the assimilation run and nature run are conducted at 4° ×5° resolution. The pseudo surface and satellite observation network are almost identical to Liu et al. (2022) but with additional ocean glint observations from the Orbiting Carbon Observatory-2 (OCO-2) (O'Dell et al., 2018; Baker et al., 2022). This kind of observation network was usually called LNLGOGIS in the OCO-2 flux model intercomparison project (OCO2MIP) (Crowell et al., 2019; Peiro et al., 2022; Byrne et al., 2023). Then the pseudo observations in each OSSE are sampled from their corresponding nature runs and randomly perturbed based on the error scales described in Liu et al. (2022). The nature runs start from the same initial CO_2 concentration and are forced by identical surface carbon fluxes with the F_{FE} from the Open-source Data Inventory of Anthropogenic CO_2 emissions (ODIAC) (Oda et al., 2018), the F_{IR} from Global Fire Assimilation System (GFAS) (Kaiser et al., 2012), the F_{OA} from Rödenbeck et al. (2014), and the F_{TA} generated from the terrestrial model of Simple Biosphere Model Version 4 (SiB4) (Haynes et al., 2019). To separate the impact of model resolution while with less impact from a priori fluxes, the a priori F_{TA} and F_{OA} used in the assimilation runs are similar as in the nature runs but from 4 years ago.

In addition to the two OSSEs, a real data assimilation experiment (EXP-real) is conducted at 4° ×5° resolution that assimilates the LNLGOGIS observations. And the a priori fluxes and assimilation period are identical to the nature run of EXP-biased. An ensemble of global inversion results (Ames, Baker, CSU, CT, OU, and TM5-4DVAR) within version 10 of OCO2MIP that assimilate the LNLGOGIS observations and without very tight ocean a priori constraint is used to validate the transport bias impact further (Byrne et al., 2023). Moreover, 4 a priori of "bottom-up" ocean flux products in the OCO2MIP systems are used as references.

3 Results

3.1 Land-ocean and tropic-extratropic partitioning

First, we analyze the surface CO_2 and column CO_2 (XCO_2) concentration in the nature runs of EXP-bias (Figure 1a, d) and EXP-perfect (Figure 1b, e). Even though the two nature runs are driven by the same surface fluxes (Figure S1), the biased ATM at 4° ×5° resolution tends to trap the CO_2 fluxes within the near-surface in the Northern Hemisphere than the ATM at native 0.5° ×0.625° resolution on an annual average basis, especially in Eurasia that the biases can reach to over 2 ppm. The XCO_2 bias has clear latitudinal distribution with positive bias in the Northern (30 °N~ 90 °N) and Southern (-90 °S~ -30 °S) middle and high latitudes and negative bias near the tropics (-30 °S~ 30 °N). Moreover, the annual bias is averaged from the seasonal varying biases. In Eurasia, the positive surface bias of over 5 ppm from January to March is reversed to the negative surface bias of over -3 ppm from July to September (Figure S2, S3). The seasonal variation of XCO_2 bias is relatively smaller than the surface CO_2. The persistent dipole tropic versus extratropic bias pattern moves southward from winter to summer.

The systematic error of simulated CO_2 concentration caused by the coarse-resolution ATM is expected to cause significant bias in flux estimates. The first assimilation run of EXP-biased assimilates the "perfect" observations but uses the "biased" ATM, which is similar to the real-world scenario. Instead, the second assimilation run of EXP-perfect has no transport model error issue that assimilates the "perfect" observations and uses the "perfect" ATM. The difference in estimated fluxes between the two assimilation runs is expected to be the impact of transport error on flux estimation. Annually, the absolute value of regional land fluxes in EXP-biased is significantly larger than EXP-perfect (Figure 2a, b). In the northern mid-latitudes land area, the carbon sink is largely overestimated in EXP-biased, especially in eastern China, eastern North America, and Europe. About half of this sink is compensated by the surrounding weakened ocean sink and carbon release in the high latitude of East Siberia (Figure 2d). Moving southward, EXP-biased shows less carbon sink in the tropical ocean, South America, Australia, and Africa and more carbon sink in the Southern Ocean. Generally, relative to EXP-perfect, the transport error tends to enhance the land carbon sink by 1.23 GtC yr^{-1} and weaken the ocean carbon sink by 0.9 GtC yr^{-1}. Moreover, more carbon sink of 0.77 GtC yr^{-1} is attributed to the extratropics (-90 °S~ -23 °S and 23 °N~ 90 °N), and 0.44 GtC yr^{-1} more carbon is released from the tropics (-23 °S~ 23 °N), resulting in a global net flux bias of -0.33 GtC yr^{-1}. Due to the high computation and memory cost, we only conduct tests for 1 year. Further research on how ATM bias affects interannual flux estimation is worth investigating in the future.

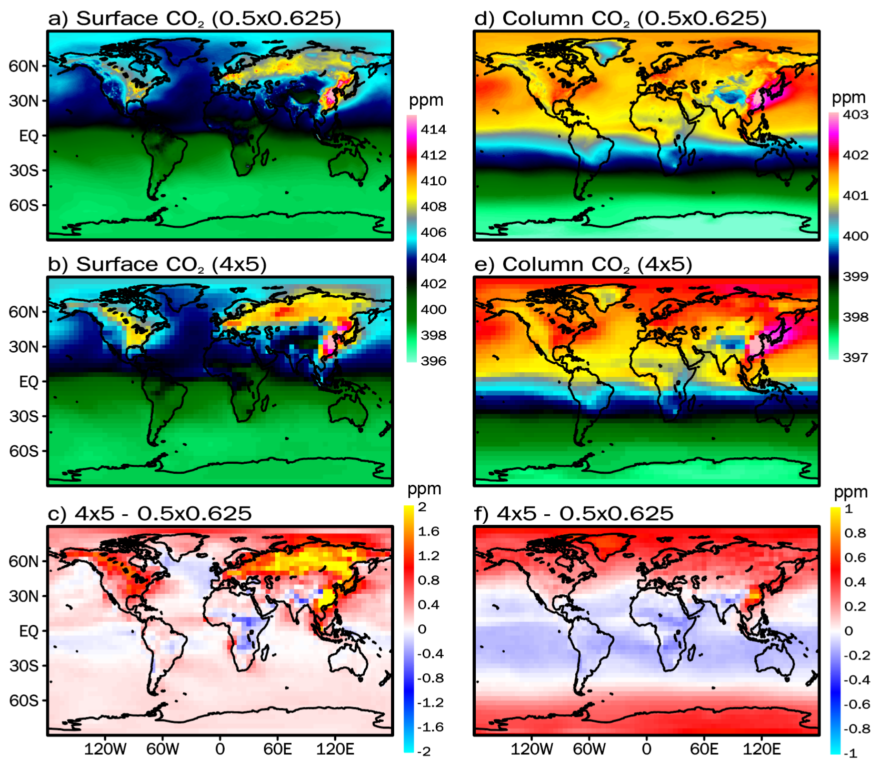

Figure 1. The annual mean surface CO_2 and column CO_2 pattern of nature runs at horizontal resolutions of 0.5°×0.625° (a, d) and 4°×5° (b, e). (c, f) The difference between the two nature runs.

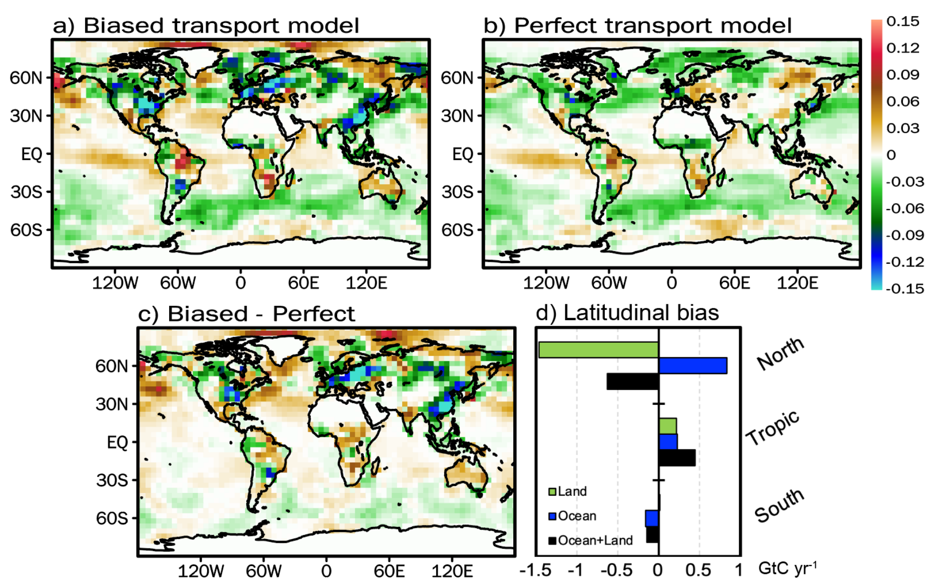

Figure 2. The spatial pattern of optimized annual mean land and ocean fluxes of assimilation runs of EXP-biased (a) and EXP-perfect (b). (c) The difference between the two assimilation runs. (d) The difference in land and ocean fluxes between the two assimilation runs in latitude bands of northern extratropics (23 °N ~ 90 °N), tropics (-23 °S ~ 23 °N), and southern extratropics (-90 °S ~ -23 °S).

3.2 Seasonal cycle

At the seasonal scale, the seasonal amplitude of the northern extratropical land flux is significantly underestimated in EXP-biased, mainly due to less carbon release during the non-growing seasons (Figure 3). In the northern extratropical ocean, the seasonal phase is reversed and the seasonal strength is enhanced, which partly compensates for the weakened seasonal amplitude in the northern extratropical land. The seasonal biases are smaller in the tropics and southern extratropics. From January to May, a large amount of carbon is released from the northern ocean. And the relative impact of transport error on the ocean flux is significantly larger than the land flux, implying that the ocean flux estimation in the context of the transport error may not be better than those a priori estimations. To overcome this limitation, inverse modelers usually apply tight a priori constraints on ocean flux in the real-world scenario (Peylin et al., 2013).

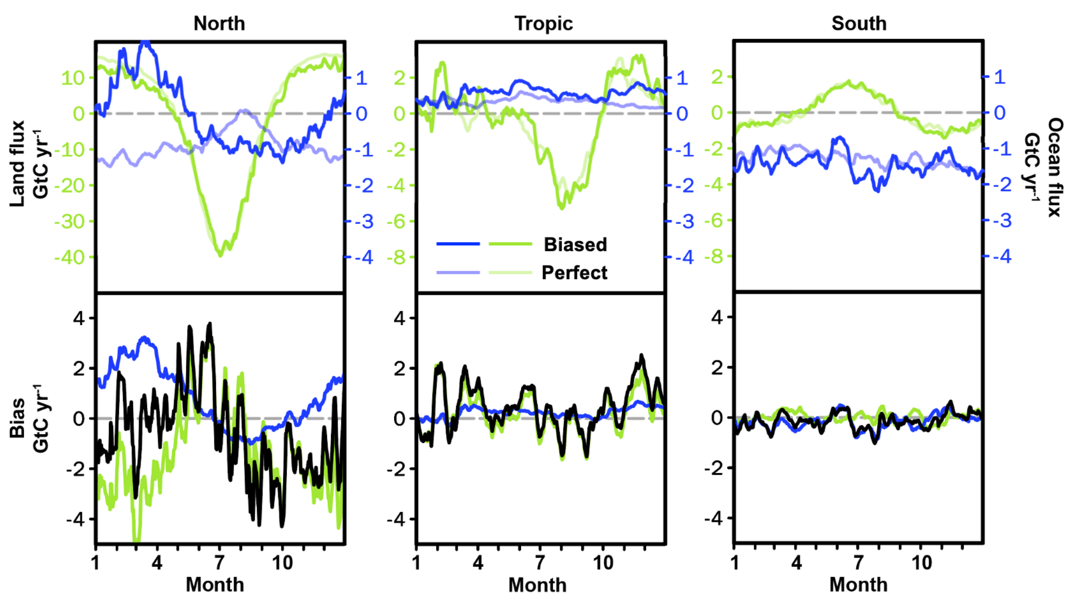

Figure 3. The upper figures are the seasonal cycle of land (green) and ocean (blue) fluxes of EXP-biased (darker color) and EXP-perfect (lighter color) at daily timestep in latitude bands of northern extratropics (23 °N ~ 90 °N), tropics (-23 °S ~ 23 °N), and southern extratropics (-90 °S ~ -23 °S). The bottom figures are the land, ocean, and net (black) fluxes difference between EXP-biased and EXP-perfect.

Global inversion systems were usually run at a coarse horizontal resolution of 2° to 5°, which is around an order of magnitude coarser than the native resolution of state-of-the-art meteorology reanalysis. Thus, the transport error is expected to significantly affect the flux estimation in the global inversions. As indicated in the OSSEs, the northern ocean is one of the regions that can be strongly affected by the transport bias. We further investigate it using real data assimilation results. A priori of process understanding and oceanic pCO_2 observations in the northern ocean provide a tight constraint on seasonal phase and amplitude of flux (Figure 4a). However, the a posteriori estimates from the 6 OCO2MIP inversion systems in the northern ocean diverge greatly during the non-growing seasons of the land biosphere, and the sink during these seasons is significantly reduced (Figure 4b). It is worth noting that the seasonal phase of the a posteriori in the CSU system and EXP-real is almost reversed from the a priori estimates. These seasonal increments from the a priori to the a posteriori are remarkably consistent in phase and magnitude with the ATM-induced flux bias in EXP-biased, indicating that the ATM bias highly influences current inversion estimates of ocean carbon fluxes. The temporal correlation between the flux bias in EXP-biased and the flux increment in EXP-real and CSU is 0.82 and 0.87, respectively. The increments in some inversion systems may not be as significant as in EXP-real and CSU, which may be because of the different degrees of constraints from the a priori.

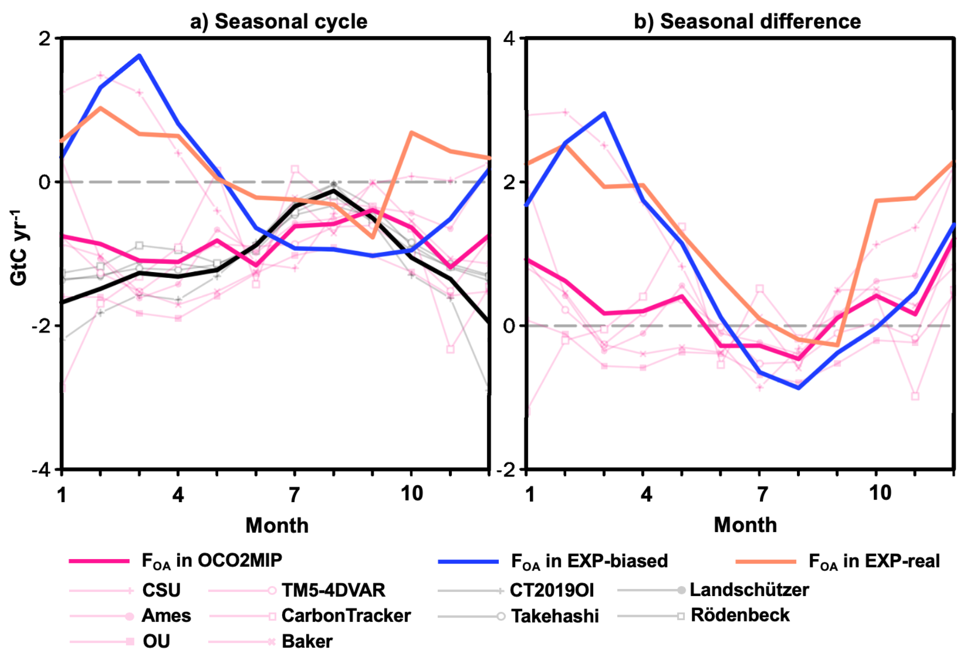

Figure 4. (a) The seasonal cycle in the northern extratropical ocean. The blue line is the a posteriori flux in EXP-biased. The orange line is the a posteriori flux in EXP-real. The dark pink line is the a posteriori flux of the ensemble mean of OCO2MIP systems. The thin pink lines with different markers are the individual a posteriori fluxes within the OCO2MIP systems. The black line is the ensemble mean of the a priori fluxes used in the different OCO2MIP systems. The thin gray lines are the individual a priori fluxes used in the OCO2MIP systems. (b) The difference compared with the ensemble mean of the a priori fluxes.

4 Discussion and conclusion

Robust regional carbon fluxes estimate is urgently needed within the framework of the United Nations Framework Convention on Climate Change and is possible as more ground greenhouse gas stations and satellites are available in the future (Kuhlmann et al., 2020). However, in the context of OSSEs, this study suggests that the coarse ATM attributes significantly more carbon uptake in the land and extratropics than in the ocean and tropics. And the seasonal amplitude in the northern land area is underestimated, which is consistent with a recent finding using aircraft observations (Cui et al., 2022). These robust pieces of evidence indicate that previous inversion studies may largely overestimate the carbon sinks in northern extratropical countries.

Focusing on the northern extratropical ocean, we find that the seasonal phase of the a posteriori fluxes totally reverses from the a priori fluxes, compensating for the reduced seasonal amplitude in the northern land area. The reversed phase is also shown in a real data assimilation experiment and some state-of-the-art inversion systems within the OCO2MIP, which is impossible from a process understanding perspective. Satellite observations over the ocean have long been argued to be biased due to retrieval algorithm bias, and inversion modelers usually discard these observations and set tight a priori ocean flux constraints (Peylin et al., 2013; Crowell et al., 2019; Palmer et al., 2019; Peiro et al., 2022). Our finding indicates that the current satellite retrieval algorithm may not be as biased as previously argued, and increasing the resolution of ATM or improving the parameterization schemes of ATM should be placed at a high priority in order to derive a robust country-level carbon budget and reasonable ocean carbon cycle estimates. Recent efforts of speeding up ATMs using Graphics Processing Units (GPU) (Chevallier et al., 2023) and Message Passing Interface (MPI) (Martin et al., 2022) Parallelization are ongoing that native resolution inversion is computationally possible in the coming years.

Acknowledgments

We are grateful to the OCO-2 Flux MIP colleagues for their valuable feedback. We thank Andrew Schuh for the suggestions and comments. This work was supported by the National Natural Science Foundation of China (No. 41975050), the project of “Monitoring, inversion and inventory joint assessment of carbon emissions in typical industrial parks under dual-carbon background” (2022ZJYF001), and the National Key R&D Program of China (grant no. 2017YFB0504000).

Conflict of Interest

The authors declare no competing interests.

Data Availability Statement

The OSSE results can be accessed at https://doi.org/10.5281/zenodo.7826041. The OCO2MIP inversion results can be accessed from: https://gml.noaa.gov/ccgg/OCO2_v10mip/download.php. The codes related to the COLA can be accessed at https://doi.org/10.5281/zenodo.7592827 and https://doi.org/10.5281/zenodo.5746140.

References

Baker, D. F., Bell, E., Davis, K. J., Campbell, J. F., Lin, B., & Dobler, J. (2022). A new exponentially decaying error correlation model for assimilating OCO-2 column-average CO2 data using a length scale computed from airborne lidar measurements. *Geoscientific Model Development*, *15*(2), 649–668. https://doi.org/10.5194/gmd-15-649-2022

Basu, S., Baker, D. F., Chevallier, F., Patra, P. K., Liu, J., & Miller, J. B. (2018). The impact of transport model differences on CO_2 surface flux estimates from OCO-2 retrievals of column average CO_2. *Atmospheric Chemistry and Physics*, *18*(10), 7189–7215. https://doi.org/10.5194/acp-18-7189-2018

Byrne, B., Baker, D. F., Basu, S., Bertolacci, M., Bowman, K. W., Carroll, D., Chatterjee, A., Chevallier, F., Ciais, P., Cressie, N., Crisp, D., Crowell, S., Deng, F., Deng, Z., Deutscher, N. M., Dubey, M. K., Feng, S., García, O. E., Griffith, D. W. T., … Zeng, N. (2023). National CO_2 budgets (2015–2020) inferred from atmospheric CO_2 observations in support of the global stocktake. *Earth System Science Data*, *15*(2), 963–1004. https://doi.org/10.5194/essd-15-963-2023

Chevallier, F. (2021). Fluxes of Carbon Dioxide From Managed Ecosystems Estimated by National Inventories Compared to Atmospheric Inverse Modeling. *Geophysical Research Letters*, *48*(15). https://doi.org/10.1029/2021GL093565

Chevallier, F., Lloret, Z., Cozic, A., Takache, S., & Remaud, M. (2023). Toward High-Resolution Global Atmospheric Inverse Modeling Using Graphics Accelerators. *Geophysical Research Letters*, *50*(5), e2022GL102135. https://doi.org/10.1029/2022GL102135

Crowell, S., Baker, D., Schuh, A., Basu, S., Jacobson, A. R., Chevallier, F., Liu, J., Deng, F., Feng, L., McKain, K., Chatterjee, A., Miller, J. B., Stephens, B. B., Eldering, A., Crisp, D., Schimel, D., Nassar, R., O'Dell, C. W., Oda, T., … Jones, D. B. A. (2019). The 2015–2016 carbon cycle as seen from OCO-2 and the global in situ network. *Atmospheric Chemistry and Physics*, *19*(15), 9797–9831. https://doi.org/10.5194/acp-19-9797-2019

Cui, Y. Y., Zhang, L., Jacobson, A. R., Johnson, M. S., Philip, S., Baker, D., Chevallier, F., Schuh, A. E., Liu, J., Crowell, S., Peiro, H. E., Deng, F., Basu, S., & Davis, K. J. (2022). Evaluating Global Atmospheric Inversions of Terrestrial Net Ecosystem Exchange CO_2 Over North America on Seasonal and Sub-Continental Scales. *Geophysical Research Letters*, *49*(18). https://doi.org/10.1029/2022GL100147

Deng, Z., Ciais, P., Tzompa-Sosa, Z. A., Saunois, M., Qiu, C., Tan, C., Sun, T., Ke, P., Cui, Y., Tanaka, K., Lin, X., Thompson, R. L., Tian, H., Yao, Y., Huang, Y., Lauerwald, R., Jain, A. K., Xu, X., Bastos, A., … Chevallier, F. (2022). Comparing national greenhouse gas budgets reported in UNFCCC inventories against atmospheric inversions. *Earth System Science Data*, *14*(4), 1639–1675. https://doi.org/10.5194/essd-14-1639-2022

Friedlingstein, P., Jones, M. W., O'Sullivan, M., Andrew, R. M., Bakker, D. C. E., Hauck, J., Le Quéré, C., Peters, G. P., Peters, W., Pongratz, J., Sitch, S., Canadell, J. G., Ciais, P., Jackson, R. B., Alin, S. R., Anthoni, P., Bates, N. R., Becker, M., Bellouin, N., … Zeng, J. (2022). Global Carbon Budget 2021. *Earth System Science Data*, *14*(4), 1917–2005. https://doi.org/10.5194/essd-14-1917-2022

Fu, Y., Liao, H., Tian, X., Gao, H., Jia, B., & Han, R. (2021). Impact of Prior Terrestrial Carbon Fluxes on Simulations of Atmospheric CO_2 Concentrations. *Journal of Geophysical Research: Atmospheres*, *126*(18). https://doi.org/10.1029/2021JD034794

Gelaro, R., McCarty, W., Suárez, M. J., Todling, R., Molod, A., Takacs, L., Randles, C. A., Darmenov, A., Bosilovich, M. G., Reichle, R., Wargan, K., Coy, L., Cullather, R., Draper, C., Akella, S., Buchard, V., Conaty, A., da Silva, A. M., Gu, W., … Zhao, B. (2017). The Modern-Era Retrospective Analysis for Research and Applications, Version 2 (MERRA-2). *Journal of Climate*, *30*(14), 5419–5454. https://doi.org/10.1175/JCLI-D-16-0758.1

Haynes, K. D., Baker, I. T., Denning, A. S., Stöckli, R., Schaefer, K., Lokupitiya, E. Y., & Haynes, J. M. (2019). Representing Grasslands Using Dynamic Prognostic Phenology Based on Biological Growth Stages: 1. Implementation in the Simple Biosphere Model (SiB4).

Journal of Advances in Modeling Earth Systems, *11*(12), 4423–4439. https://doi.org/10.1029/2018MS001540
Jiang, F., He, W., Ju, W., Wang, H., Wu, M., Wang, J., Feng, S., Zhang, L., & Chen, J. M. (2022). The status of carbon neutrality of the world's top 5 CO2 emitters as seen by carbon satellites. *Fundamental Research*, *2*(3), 357–366. https://doi.org/10.1016/j.fmre.2022.02.001
Kaiser, J. W., Heil, A., Andreae, M. O., Benedetti, A., Chubarova, N., Jones, L., Morcrette, J.-J., Razinger, M., Schultz, M. G., Suttie, M., & van der Werf, G. R. (2012). Biomass burning emissions estimated with a global fire assimilation system based on observed fire radiative power. *Biogeosciences*, *9*(1), 527–554. https://doi.org/10.5194/bg-9-527-2012
Kuhlmann, G., Brunner, D., Broquet, G., & Meijer, Y. (2020). Quantifying CO2 emissions of a city with the Copernicus Anthropogenic CO2 Monitoring satellite mission. *Atmospheric Measurement Techniques*, *13*(12), 6733–6754. https://doi.org/10.5194/amt-13-6733-2020
Liu, J., Fung, I., Kalnay, E., & Kang, J.-S. (2011). CO_2 transport uncertainties from the uncertainties in meteorological fields. *Geophysical Research Letters*, *38*, L12808. https://doi.org/10.1029/2011GL047213
Liu, Z., Zeng, N., Liu, Y., Kalnay, E., Asrar, G., Cai, Q., & Han, P. (2023). *Assimilating the dynamic spatial gradient of a bottom-up carbon flux estimation as a unique observation in COLA (v2.0)*. https://doi.org/10.5194/gmd-2023-15
Liu, Z., Zeng, N., Liu, Y., Kalnay, E., Asrar, G., Wu, B., Cai, Q., Liu, D., & Han, P. (2022). Improving the joint estimation of CO2 and surface carbon fluxes using a constrained ensemble Kalman filter in COLA (v1.0). *Geosci. Model Dev.*, *15*, 5511–5528. https://doi.org/10.5194/gmd-15-5511-2022
Martin, R. V., Eastham, S. D., Bindle, L., Lundgren, E. W., Clune, T. L., Keller, C. A., Downs, W., Zhang, D., Lucchesi, R. A., Sulprizio, M. P., Yantosca, R. M., Li, Y., Estrada, L., Putman, W. M., Auer, B. M., Trayanov, A. L., Pawson, S., & Jacob, D. J. (2022). Improved advection, resolution, performance, and community access in the new generation (version 13) of the high-performance GEOS-Chem global atmospheric chemistry model (GCHP). *Geoscientific Model Development*, *15*(23), 8731–8748. https://doi.org/10.5194/gmd-15-8731-2022
Oda, T., Maksyutov, S., & Andres, R. J. (2018). The Open-source Data Inventory for Anthropogenic CO_2, version 2016 (ODIAC2016): A global monthly fossil fuel CO_2 gridded emissions data product for tracer transport simulations and surface flux inversions. *Earth System Science Data*, *10*(1), 87–107. https://doi.org/10.5194/essd-10-87-2018
O'Dell, C. W., Eldering, A., Wennberg, P. O., Crisp, D., Gunson, M. R., Fisher, B., Frankenberg, C., Kiel, M., Lindqvist, H., Mandrake, L., Merrelli, A., Natraj, V., Nelson, R. R., Osterman, G. B., Payne, V. H., Taylor, T. E., Wunch, D., Drouin, B. J., Oyafuso, F., … Velazco, V. A. (2018). Improved retrievals of carbon dioxide from Orbiting Carbon Observatory-2 with the version 8 ACOS algorithm. *Atmospheric Measurement Techniques*, *11*(12), 6539–6576. https://doi.org/10.5194/amt-11-6539-2018
Palmer, P. I., Feng, L., Baker, D., Chevallier, F., Bösch, H., & Somkuti, P. (2019). Net carbon emissions from African biosphere dominate pan-tropical atmospheric CO2 signal. *Nature Communications*, *10*(1), 3344. https://doi.org/10.1038/s41467-019-11097-w
Peiro, H., Crowell, S., Schuh, A., Baker, D. F., O'Dell, C., Jacobson, A. R., Chevallier, F., Liu, J., Eldering, A., Crisp, D., Deng, F., Weir, B., Basu, S., Johnson, M. S., Philip, S., & Baker, I. (2022). Four years of global carbon cycle observed from the Orbiting Carbon Observatory 2 (OCO-2) version 9 and in situ data and comparison to OCO-2 version 7. *Atmospheric Chemistry and Physics*, *22*(2), 1097–1130. https://doi.org/10.5194/acp-22-1097-2022

Peylin, P., Law, R. M., Gurney, K. R., Chevallier, F., Jacobson, A. R., Maki, T., Niwa, Y., Patra, P. K., Peters, W., Rayner, P. J., Rödenbeck, C., van der Laan-Luijkx, I. T., & Zhang, X. (2013). Global atmospheric carbon budget: Results from an ensemble of atmospheric CO₂ inversions. *Biogeosciences*, *10*(10), 6699–6720. https://doi.org/10.5194/bg-10-6699-2013

Philip, S., Johnson, M. S., Potter, C., Genovesse, V., Baker, D. F., Haynes, K. D., Henze, D. K., Liu, J., & Poulter, B. (2019). Prior biosphere model impact on global terrestrial CO_2 fluxes estimated from OCO-2 retrievals. *Atmospheric Chemistry and Physics*, *19*(20), 13267–13287. https://doi.org/10.5194/acp-19-13267-2019

Rödenbeck, C., Bakker, D. C. E., Metzl, N., Olsen, A., Sabine, C., Cassar, N., Reum, F., Keeling, R. F., & Heimann, M. (2014). Interannual sea–air CO2 flux variability from an observation-driven ocean mixed-layer scheme. *Biogeosciences*, *11*(17), 4599–4613. https://doi.org/10.5194/bg-11-4599-2014

Schimel, D., Stephens, B. B., & Fisher, J. B. (2015). Effect of increasing CO_2 on the terrestrial carbon cycle. *Proceedings of the National Academy of Sciences*, *112*(2), 436–441. https://doi.org/10.1073/pnas.1407302112

Schuh, A. E., Byrne, B., Jacobson, A. R., Crowell, S. M. R., Deng, F., Baker, D. F., Johnson, M. S., Philip, S., & Weir, B. (2022). On the role of atmospheric model transport uncertainty in estimating the Chinese land carbon sink. *Nature*, *603*(7901), E13–E14. https://doi.org/10.1038/s41586-021-04258-9

Schuh, A. E., & Jacobson, A. R. (2022). Uncertainty in Parameterized Convection Remains a Key Obstacle for Estimating Surface Fluxes of Carbon Dioxide. *Atmospheric Chemistry and Physics Discussion [Preprint]*. https://doi.org/10.5194/acp-2022-616

Schuh, A. E., Jacobson, A. R., Basu, S., Weir, B., Baker, D., Bowman, K., Chevallier, F., Crowell, S., Davis, K. J., Deng, F., Denning, S., Feng, L., Jones, D., Liu, J., & Palmer, P. I. (2019). Quantifying the Impact of Atmospheric Transport Uncertainty on CO_2 Surface Flux Estimates. *Global Biogeochemical Cycles*, *33*(4), 484–500. https://doi.org/10.1029/2018GB006086

Stephens, B. B., Gurney, K. R., Tans, P. P., Sweeney, C., Peters, W., Bruhwiler, L., Ciais, P., Ramonet, M., Bousquet, P., Nakazawa, T., Aoki, S., Machida, T., Inoue, G., Vinnichenko, N., Lloyd, J., Jordan, A., Heimann, M., Shibistova, O., Langenfelds, R. L., … Denning, A. S. (2007). Weak Northern and Strong Tropical Land Carbon Uptake from Vertical Profiles of Atmospheric CO_2. *Science*, *316*(5832), 1732–1735. https://doi.org/10.1126/science.1137004

The International GEOS-Chem User Community. (2021). *geoschem/GCClassic: GEOS-Chem 13.0.2* (13.0.2). Zenodo. https://doi.org/10.5281/ZENODO.4681204

Wang, J., Feng, L., Palmer, P. I., Liu, Y., Fang, S., Bösch, H., O'Dell, C. W., Tang, X., Yang, D., Liu, L., & Xia, C. (2020). Large Chinese land carbon sink estimated from atmospheric carbon dioxide data. *Nature*, *586*(7831), 720–723. https://doi.org/10.1038/s41586-020-2849-9

Weir, B., Oda, T., Ott, L. E., & Schmidt, G. A. (2022). Assessing progress toward the Paris Climate Agreement from Space. *Environmental Research Letters*. https://doi.org/10.1088/1748-9326/ac998c

Yu, K., Keller, C. A., Jacob, D. J., Molod, A. M., Eastham, S. D., & Long, M. S. (2018). Errors and improvements in the use of archived meteorological data for chemical transport modeling: An analysis using GEOS-Chem v11-01 driven by GEOS-5 meteorology. *Geoscientific Model Development*, *11*(1), 305–319. https://doi.org/10.5194/gmd-11-305-2018